Integrated solar capacitors for energy conversion and storage

Ruiyuan Liu^{1,2}, Yuqiang Liu¹, Haiyang Zou², Tao Song¹ (🖂), and Baoquan Sun¹ (🖂)

Received: 28 October 2016 Revised: 30 December 2016 Accepted: 2 January 2017

© Tsinghua University Press and Springer-Verlag Berlin Heidelberg 2017

KEYWORDS

solar cell, supercapacitor, energy conversion and storage, integrated devices

ABSTRACT

Solar energy is one of the most popular clean energy sources and is a promising alternative to fulfill the increasing energy demands of modern society. Solar cells have long been under intensive research attention for harvesting energy from sunlight with a high power-conversion efficiency and low cost. However, the power outputs of photovoltaic devices suffer from fluctuations due to the intermittent instinct of the solar radiation. Integrating solar cells and energy-storage devices as self-powering systems may solve this problem through the simultaneous storage of the electricity and manipulation of the energy output. This review summarizes the research progress in the integration of new-generation solar cells with supercapacitors, with emphasis on the structures, materials, performance, and new design features. The current challenges and future prospects are discussed with the aim of expanding research and development in this field.

1 Introduction

The considerable developments in modern electronics raise the demand for sustainable technologies achieved by integrating energy harvesting and storage functions in a single device as a self-powering unit. Different integrated devices based on the conversion of solar, mechanical, or thermal energy by energy-harvesting parts and the direct charging of energy-storage parts have been developed during the past decades [1–7]. As an unlimited, widespread, and renewable clean resource, solar energy has long been a promising alternative to conventional fossil fuel. Silicon solar

cells are by far the most successful commercialized photovoltaic devices and dominate more than 90% of the solar-cell market. However, they are rigid devices with a complicated fabrication process, which hinders their application in flexible and portable electronics. New-generation solar cells, including dye-sensitized solar cells (DSSCs), organic solar cells (OSCs), and the recently emerging perovskite solar cells (PVSCs), have the advantages of high efficiency, easy fabrication, low cost, and flexibility [8–18]. The integration of solar cells with energy-storage parts not only realizes solar energy storage but also can diminish the fluctuation of light illumination as the power output source.

Address correspondence to Tao Song, tsong@suda.edu.cn; Baoquan Sun, bqsun@suda.edu.cn



¹ Jiangsu Key Laboratory for Carbon-Based Functional Materials and Devices, Institute of Functional Nano and Soft Materials (FUNSOM) and Collaborative Innovation Center of Suzhou Nano Science and Technology, Soochow University, Suzhou 215123, China

² School of Materials Science and Engineering, Georgia Institute of Technology, Atlanta, GA 30332-0245, USA

Electrochemical systems, including batteries and electrochemical supercapacitors, designed for energy storage are especially favored because they are sustainable and eco-friendly [19-20]. Among these, supercapacitors are outstanding owing to their high power density, relatively low weight, quick response to potential changes, long cycle life, and long-term stability [21-23]. Thus, self-powering systems comprising solar cells for energy conversion and supercapacitors for energy storage have been popular in the past few years. On one hand, novel-configuration devices based on different materials are necessary to improve the electrical performance of the integrated system, such as the power-conversion efficiency (PCE) of the solar cells and the energy-storage ability of the supercapacitors, to satisfy the increasing energy requirements of next-generation electronic devices. On the other hand, special properties, e.g., stretchable, flexible, bendable, smart, and transparent, have been well explored for expanding the applications of devices in portable or wearable electronics [24-27]. The printable property, which is compatible with the roll-to-roll process, offers the opportunity for directly integrating thin and flexible energy functions with printed devices [3]. Fiber-shaped solar cells and supercapacitors are promising for weaving multifunctional smart clothes. A smart integrated device can have an automatically tunable optical transmittance during the photocharging process [28].

In this review, we briefly summarize the recent developments of new-generation solar cells integrated with supercapacitors, hereinafter called solar capacitors. An overview of the operating mechanism and configurations of the integrated system is first presented. The state-of-the-art research progress in solar capacitors based on different solar cells and supercapacitors, including their design configuration, electrode fabrication, and device performance, is then summarized. Finally, the current challenges and prospects for future research are discussed.

2 Overview of integrated solar capacitors

There are two main configurations of the integrated device: the traditional planar structure and the newly emerging fiber-shaped one. The integration of the solar energy conversion part and the electrical storage part can be realized either in one device or by sharing a common electrode as a connection. A completed solar capacitor should consist of a front electrode for the solar cell and a counter electrode for the supercapacitor. Various kinds of solar cells, including silicon solar cells, DSSCs, OSCs, and PVSCs, have been successfully integrated with supercapacitors to fabricate self-charging energy units. Upon light illumination, the solar cell converts solar energy into electrical energy and charges the supercapacitor, which is usually described as a photocharging process. The discharging process occurs when the capacitors are connected with an external load to supply power, either under light or in the dark.

2.1 Performance evaluation for integrated solar capacitors

The overall efficiency of the integrated device is determined by the photovoltaic energy conversion part and the electrochemical energy-storage one. The electrical resistance between these parts significantly affects the overall device efficiency. The electrical resistance can be calculated either by multiplying the PCE of the solar cell and the storage efficiency of the supercapacitors or by dividing the energy of the illuminated light by the energy stored during the photocharging process.

The PCE of a solar cell under light illumination is calculated using the following equation

$$PCE = V_{oc} J_{sc} FF / P_{in}$$
 (1)

where $V_{\rm oc}$ $J_{\rm sc}$ FF, and $P_{\rm in}$ are the open-circuit voltage, the short-circuit current density, the fill factor, and the incident-light power density (100 mW/cm²), respectively. The energy of the light ($E_{\rm light}$) illuminating the solar cell during the photocharging time (t, s) per unit area is calculated using the equation

$$E_{\text{light}} = P_{\text{in}} t \tag{2}$$

Typically, to evaluate the performance of supercapacitors, cyclic-voltammetry tests at different scan rates are performed, and galvanostatic charge/discharge curves at different current densities, as well as electrochemical impedance spectra, are obtained. The capacitance (C, F) and areal specific capacitance (C_A, F/cm²) can be derived from the charge or discharge curve according to the following equations

$$C = I dt/dV (3)$$

$$C_{\rm A} = C/A \tag{4}$$

where I (A) is the current, t (s) is the time, and V (V) is the potential window in the charge/discharge process, respectively. A (cm²) is the area of the tested device.

The stored energy (E_{storage} , W), areal energy density (E_{A} , Wh/cm²), and power density (P_{A} , W/cm²) of the supercapacitor during the charging process are calculated using the following equations

$$E_{\text{storage}} = 0.5CV^2 \tag{5}$$

$$E_{\rm A} = 0.5C_{\rm A}V^2/3600 = C_{\rm A}V^2/7200$$
 (6)

$$P_{\mathsf{A}} = E_{\mathsf{A}}/3600t \tag{7}$$

The overall efficiency (η_{overall}) of the integrated device can be obtained according to the following equation

$$\eta_{\text{overall}} = E_{\text{storage}} / (E_{\text{light}} A_{\text{solar}})$$
(8)

where A_{solar} (cm²) is the area of the solar cell [29, 30].

2.2 Planar integrated devices

Along with the development of solar cells, the concept of planar solar conversion and storage integrated devices emerged as early as 1970s. Hodes et al. reported a corrosion-free CdSe photoelectrochemical cell with a novel extension that allowed the in situ storage of the converted solar energy [31]. In the photocharging process, CdSe was excited under light radiation higher than its bandgap energy, inducing photogenerated carriers. The holes were injected into the S/S²⁻ cathode to oxidize the polysulfide, and the electrons were transported through external circuit to provide power and electrochemical storage by the reduction of Ag₂S to Ag on the anode. In the dark, the Ag anode was spontaneously oxidized because of the reduction of the photoelectrode, and the electrons flowed through the external load to reduce the sulfur on the cathode, which was the discharging process. Their initial design was a two-electrode device, as shown in Fig. 1(a), and the potential dropped quickly under a load, which

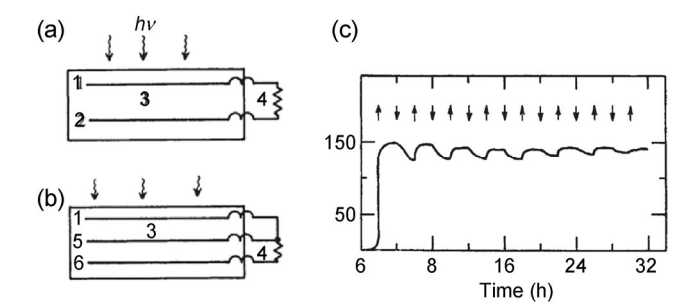


Figure 1 Configurations of the initial prototypes of the solar energy conversion and storage in devices with (a) a two-electrode system and (b) a three-electrode one. (c) Voltage–time profile for a three-electrode system with light on and off. Reproduced with permission from Ref. [31], © Nature Publishing Group 1976.

was attributed to the large resistance losses in the system. Figures 1(b) and 1(c) show a three-electrode configuration and the corresponding performance with light on and off. The cell was photocharged under light illumination and discharged in the dark with a photovoltage of 125–150 mV, but the storage efficiency was low because the storage electrode directly contacted the other electrodes. A cation-specific membrane was introduced to separate the electrodes, and sulfur was excluded from the storage compartment, yielding storage efficiencies of ~90%. The initial prototype of this integrated device was the first example of solar energy conversion and storage in a single device.

Solar capacitors achieved by integrating solar cells with capacitors in planar forms have made rapid progress in the past few years. The simplest design involves externally connecting the two independent energy parts with each other; however, this structure suffers from power loss on the resistance. The rigid connections also hinder its applications to portable electronics. In addition, this configuration does not fit the concept of "integration" for a light and compact device. An integrated device should have at least one common electrode to conduct the energy conversion and storage by either an in situ process or electron transfer. A more promising aspect of new solar cells such as OSCs is their ability to be fabricated on flexible substrates via low-temperature processing. Printable OSCs fabricated using layer-by-layer or roll-to-roll techniques have attracted considerable attention for large-scale fabrication.

2.3 Fiber-shaped integrated devices

Fiber-shaped devices are obtained by rolling up the planar structure and usually have a common electrode. The solar-cell part and the supercapacitor part should be in fiber forms and integrated in the core-shell or twisted-configuration structure. Fiber-shaped devices have unique properties and the advantages of lightness, compatibility with weaving, and flexibility, which are favored in portable and wearable electronics. Fiber solar cells have the advantage of light incident angleindependent properties compared with planar ones. Moreover, the structured surface of fiber substrates can increase the absorption from scattered and reflected light, which can significantly expand the adaptability of solar cells to the environment. An aligned TiO₂ nanotube array on a Ti wire was twisted with an aligned CNT fiber to produce an integrated energy wire [29]. The electrochemical anodized obtained TiO₂ nanotube improved the charging separation and transportation in a DSSC and increased the surface area in a supercapacitor. Two separated CNT fibers were wrapped on a Ti wire with pitches of 1.1 and 0.7 mm for the DSSC and supercapacitor parts, respectively. The PCE of the solar cell was 2.2%, with a relatively low FF arising from the high resistance induced by the poor contact between the physically twisted CNT fiber and the Ti wire. The area specific capacitance of the energy-storage part was 0.6 mF/cm², which is within the typical range of 0.4–2.0 mF/cm² for reported micro-supercapacitors. The voltage was charged to 0.6 V upon AM 1.5 G light illumination, which was somehow lower than the V_{oc} (0.68 V) in the DSSC due to the self-discharging. The overall power efficiency was calculated to be 1.5%, with an energystorage efficiency of 68.4%.

Solar cells under illumination generate heat. However, most supercapacitors have liquid or gel-like electrolytes. In general, a moderate increase in the operating temperature improves the performance of supercapacitors, mainly because of the decrease in the size of solvated ions (for liquid or gel-like electrolyte-based electrical double-layer capacitors) and the increase in the electrical conductivity of the electrolytes. The decrease in the size of solvated ions and the increase in the electrical conductivity of the electrolytes lead to a larger

specific capacitance and smaller equivalent series resistance (and higher discharge voltage), respectively, improving the energy and power densities of the supercapacitor.

3 Integrated solar capacitors with different configurations

3.1 Integrated solar capacitors based on DSSCs and supercapacitors

Since the breakthrough work by Gräztel and O'Regan in 1991, DSSCs have been extensively studied as promising alternatives to conventional solar cells [11, 32]. A typical DSSC has a sandwich structure incorporating two face-to-face electrodes—a working electrode and a counter electrode—separated by an electrolyte. The working electrode is usually a transparent glass or plastic substrate with a thin layer of transparent conducting oxide for depositing the mesoporous TiO₂ layer. Another substrate coated with a thin layer of Pt or C materials is used as a cathode. The electrolyte is usually an iodide/triiodide redox pair in an organic solvent. A monolayer of dye is attached to the surface of the working electrode for light absorption and charge transfer in the electrolyte. Upon illumination, generated electrons are injected into the conduction band of TiO₂, leaving the dye in an oxidation state. Then, electrons are collected by the anode and flow into the external part to reduce the triiodide into iodide, which releases electrons to restore the oxidized dye molecules to the ground state. In past years, the highest PCE for DSSCs was ~14%, which is comparable to that of commercialized amorphous silicon solar cells [33–35]. Owing to their low-cost and simple process, diversity of colors, and good performance under low illumination, DSSCs have become a popular energy-conversion part in integrated devices (Table 1) [1, 2, 30, 36–44].

In 2004, Miyasaka et al. reported for the first time a two-electrode integrated planar device comprising a DSSC and a supercapacitor that achieved the *in situ* conversion and storage of solar energy [1]. The device, which was called a photocapacitor, was constructed on a multilayer photoelectrode comprising dye-sensitized TiO_2 /hole-trapping layer/activated carbon particles

Table 1 Integrated solar capacitors based on solar cells and supercapacitors

Year	Device structure	Solar cell (max. PCE if provided, %)	Storage configuration	Photocharged cell voltage (V)	Overall efficiency (%)	Ref.
2004	Planar	DSSC	AC ^a /(CH ₃ CH ₂) ₄ NBF ₄ /AC	0.46	N/A	[1]
2005	Planar	DSSC	AC/(CH ₃ CH ₂) ₄ NBF ₄ /AC	0.8	N/A	[36]
2010	Planar	DSSC	PProDOT-Et ₂ /LiClO ₄ /PProDOT-Et ₂	0.75	0.6	[37]
2010	Planar	DSSC (4.37)	PEDOT/LiClO ₄ /PEDOT	0.69	N/A	[45]
2011	Fiber	DSSC (0.02)	Cu/H ₃ PO ₄ -PVA ^b /graphene	N/A	N/A	[2]
2012	Fiber	DSSC (2.5)	Ti/H ₃ PO ₄ -PVA/CNT	0.6	1.5	[29]
2013	Fiber	DSSC (5.41)	PANI-SS ^c /H ₂ SO ₄ /PANI	0.621	2.12	[38]
2013	Planar	DSSC (6.1)	MWCNT/H ₃ PO ₄ -PVA/MWCNT	0.72	5.12	[39]
2014	Planar	DSSC (3.17)	ATO ^d /LiSO ₄ /ATO	0.61	1.64	[30]
2014	Fiber	DSSC (6.47)	MWCNT/H ₃ PO ₄ -PVA/MWCNT	0.65	1.83	[40]
2015	Planar	DSSC (4.8)	Porous Si-Carbon/ PEO-EMIBF ₄ ^e /porous Si-carbon	0.64	2.1	[41]
2011	Planar	OSC (3.39)	CNT/H ₃ PO ₄ -PVA/CNT	0.6	N/A	[3]
2014	Fiber	OSC (1.01)	Ti/H ₃ PO ₄ -PVA/MWCNT	0.4	0.82	[5]
2016	Planar	OSC (7.6)	Carbon black/BMIM BF ₄ / carbon black	0.87	2.92	[46]
2015	Planar	PVSC (13.6)	BC/PPy nanofibers/MWCNTs	0.71	10	[47]
2016	Planar	PVSC (12.54)	$WO_3/PVA-H_2SO_4/WO_3$	0.68	N/A	[28]
2016	Planar	PVSC (6.37)	PEDOT-carbon/LiClO ₄ / PEDOT-carbon	0.71	4.7	[48]

^aAC: active carbon; ^bPVA: polyvinyl alcohol; ^cPANI-SS: polyaniline-stainless steel; ^dATO: anodic titanium oxide; ^ePEO: poly(ethylene-oxide).

in contact with an organic electrolyte solution, as shown in Fig. 2(a). The photoinduced positive and negative charges in the solar cells accumulated on the microporous surface of the activated carbon. The device had a charging voltage of 0.45 V, a chargedischarge Coulombic efficiency of 80%, and an area specific capacitance of 0.69 F/cm². However, the internal resistance during the discharge process was relatively large because the electrons passed through the Schottky barrier in the TiO₂ layer. To overcome this problem, the same group reported a three-electrode configuration employing an internal dual-functional Pt electrode between the previous electrodes to conduct redox electron transfer and charge storage simultaneously [36]. As shown in Fig. 2(b), the improved photocapacitor was realized with an activated-carbon layer deposited on one side of the Pt as the internal electrode. Pt-sputtered conducting glass acted as a counter electrode. In the discharging process, the electrons moved to the active carbon more efficiently on the internal electrode without the potential barrier. As a result, the internal resistance significantly decreased from 2.6 k Ω to 330 Ω compared with the two-electrode device. This three-electrode configuration exhibited an energy density per area five times higher than that of the counterpart, with a high charge-state voltage of 0.8 V. However, the Coulombic efficiency was relatively low owing to the back electron transfer at the internal electrode caused by the partial quenching of the holes that accumulated in the active carbon because of iodide anions. This configuration has become the prototype for the following integrated photocharging devices with improved electrical and mechanical properties, as well as for the fabrication process towards self-charging units.

For supercapacitors, various materials have been investigated as electrodes, such as carbon nanotubes (CNTs), graphene, metal oxides, and conducting

6 Nano Res.

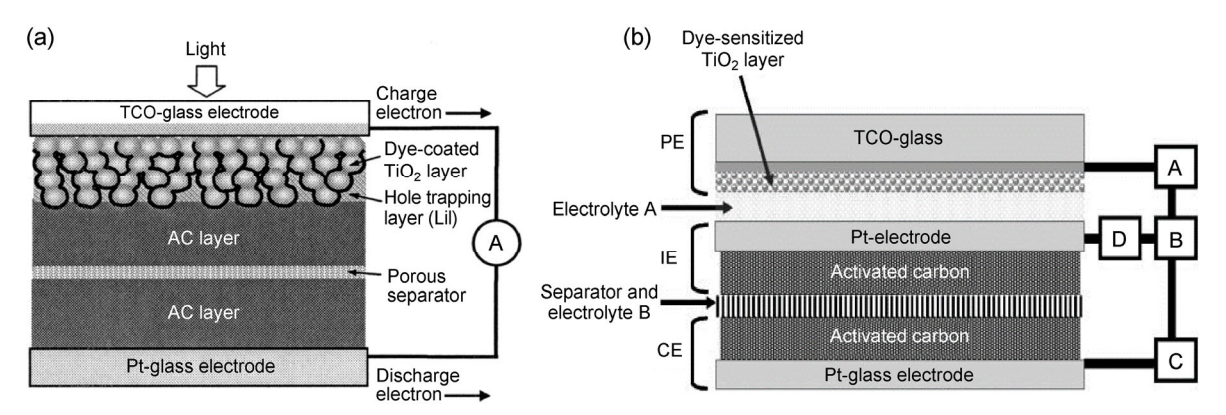


Figure 2 Schematic of the sandwich multilayer integrated device with (a) two electrodes (reproduced with permission from Ref. [1], © AIP Publishing LLC 2004) and (b) three electrodes (reproduced with permission from Ref. [36], © Royal Society of Chemistry 2005).

polymers [49-53]. Supercapacitors using CNT films as electrodes had good performances; e.g., a printable thin-film device had a gravimetric capacitance of ~120 F/g [54]. Although CNTs are widely used in DSSCs and supercapacitors, they were not effectively integrated until Peng et al. reported an all-solid-state device using freestanding and aligned multiwall CNT (MWCNT) films as co-shared electrodes [39]. The large surface area of the MWCNTs resulted in a fiber solar cell with a PCE of 6.10%, a gravimetric capacitance of 48 F/g, a storage efficiency of ~84%, and an overall efficiency of ~5.12%. Polyaniline (PANI) was incorporated into an MWCNT film to increase the gravimetric capacitance from ~26 to 208 F/g. The cyclic stability of the integrated devices was tested for over 100 cycles, during which the discharge capacitances of the bare MWCNT remained nearly constant. More recently, an individual crystal silicon substrate was integrated into a multifunctional platform, where one side served as the photocathode of the DSSC and the other side provided onboard charge storage for the supercapacitor [41]. A two-step process was implemented to transform the silicon substrate: the doubled-sided electrochemical fabrication of porous silicon and the thermal carbon passivation catalyzed by the porous silicon. The silicon substrate simultaneously provided Faradaic charge transfer for a DSSC as well as non-Faradaic double-layer charge storage for the supercapacitor. The device stored 80% of the energy in 1.2 s and achieved an overall efficiency of 2.1%. Compared with other reports, silicon was used for both the energy storage and conversion electrodes. This eliminated the need for Pt in the DSSC, which may enable the large-scale application of the integrated device. Additionally, a CdS/CdSe quantum-dot DSSC was integrated with a mesh-based carbon supercapacitor by a shared double-sided mesh-typed electrode [55].

Conducting polymers, such as polypyrrole (PPy), polythiophene, and poly(3,4-ethylenedioxythiophene) (PEDOT) are popular capacitor materials that undergo a fast redox reaction to provide a capacitive response with a higher power capability [49, 50]. Ho et al. proposed a flexible integrated solar capacitor combining 0.5 mm-thick PEDOT and a dye N710-TiO₂ photoactive layer [45]. The plastic-based DSSC had an overall efficiency of 4.37% with an 11-µm-thick TiO₂ photoanode. The supercapacitor provided an area specific capacitance of 0.52 F/cm². They also reported another polymer-based solar capacitor device using an N3-dye adsorbed photoelectrode and poly(3,3diethyl-3,4-dihydro-2H-thieno-[3,4-b] [1,4] dioxepine) (PProDPT-Et₂) films as a capacitor electrode. This device achieved an area-specific capacitance of 0.48 F/cm² and a photocharged voltage of 0.75 V, with an overall efficiency of 0.6% [37]. PEDOT exhibited a slightly higher mass specific capacitance than PProDOT-Et₂ because of the smaller molar mass of the monomer. However, the latter had a higher specific capacitance with a porous thick film. Jiang et al. modified the counter electrodes of DSSCs by using poly (vinylidene fluoride) (PVDF)/ZnO nanowire array nanocomposites for energy storage. The stored charge density was as high as 2.14 C/g, and the overall efficiency of the

device was as high as 3.70% [44].

In addition to carbon-based materials and polymers, metal oxide has been utilized as a capacitor material. Kulesza et al. integrated a solid-state DSSC with ruthenium oxide as a charge-storage material into a solar capacitor [56]. Ruthenium oxide is widely known as a mixed-valence redox conducting material with fast charge transportation in solids [57]. The threeelectrode planar electrodes included a conjugated polymer layer of poly-(3-hexylthiophene-2,5-diyl) (P3HT) for the DSSC and an evaporated silver electrode as an intermediate bipolar electrode. The device yielded a Coulombic efficiency of 88% and an overall efficiency of 0.8% under light illumination, with an area specific capacitance as high as 3.26 F/cm². Li et al. reported an anodic TiO₂ nanotube array-based integrated thinfilm device with an overall efficiency of 1.61% [30]. Plasma-assisted hydrogenation treatment was conducted on TiO₂ nanotube films to increase the electrode surface area, enhancing the capacitance in the storage device. As a result, the areal specific capacitance increased from 0.215 to 1.1 mF/cm².

Wang et al. reported the first fiber system that could simultaneously harvest both solar and mechanical energy, which were both stored in a nanowire-based supercapacitor [2]. The multifunctional power fiber consisted of a ZnO nanowire piezoelectric nanogenerator, a DSSC, and a supercapacitor. ZnO nanowires were radially synthesized on a single polymethyl-methacrylate layer as the acting units for the nanogenerator to scavenge mechanical energy, as well as for the core of the solar cell and the large-area supercapacitor. Graphene on a Cu mesh was wrapped around the plastic wire used as cylindrical electrodes for the three units. The maximum output current and $V_{\rm oc}$ of the nanogenerator with a strain of ~0.1% were 2 nA and 7 mV, respectively. The fiber-shaped DSSC exhibited a J_{sc} of 0.35 mA/cm², a V_{oc} of 0.17 V, and an FF of 0.39, yielding a PCE of 0.02%. The low PCE was attributed to the poor transparency of the Cu mesh, which resulted in a low I_{sc} . The solid gel electrolytebased supercapacitor showed a linear specific capacitance of 0.025 mF/cm. This device used graphene as an electrode and a ZnO nanowire for the nanogenerator and DSSC. However, the fabrication process was relatively complicated. In addition, the graphene on the Cu mesh reduced the electrode transparency, decreasing the light-harvesting capability of the DSSC.

Another integrated power fiber with a similar configuration was reported in 2013 [38]. A stainlesssteel wire coated with PANI was used as the common electrode of the DSSC and supercapacitor. A Ti wire was coated with a TiO₂ layer as the photoanode. The two fiber electrodes were sealed in parallel in a tube filled with liquid electrolytes (Fig. 3). The PCE of the PANI-based fiber-shaped DSSC was as high as 5.41%, and the area specific capacitance of the supercapacitor was 41 mF/cm², which is almost two orders of magnitude higher than that in previous reports. The overall efficiency of the integrated power fiber was as high as 2.1%. Compared with previous reports, this device achieved high energy conversion and storage efficiencies and has an inexpensive and facile manufacture process [2]. TiO₂ was coated as an anode instead of the ZnO nanowire, increasing the chemical stability. However, the two-wire structure still suffered from the disadvantages of electrode separation and liquid-electrolyte leakage under bending.

Compared with the two-wire devices, which usually suffer from a high internal resistance, the single wirebased core-shell integrated system might overcome this issue. Peng et al. developed a novel coaxial energy fiber based on a Ti wire modified with vertically aligned TiO₂ nanotubes on the surface and a horizontally aligned MWCNT sheet serving as the two electrodes (Fig. 4) [58]. The TiO₂ modified Ti wire was the common electrode for the DSSC and supercapacitor, and CNT sheets were wrapped onto the Ti wire as the other electrode. To solve the leakage problem, they fabricated an all-solid-state device, for which a melted solid-state electrolyte was used for the DSSC and gel PVA/H₃PO₄ coated on a TiO2-modified Ti wire was used as the electrolyte of the supercapacitor. The DSSC achieved a PCE of 2.73%, and the energy-storage efficiency of the integrated fiber device reached 75.7% with an area specific capacitance as high as 3.32 mF/cm² and power densities as high as 0.013 mW/cm (0.27 mW/cm²) at a current of 50 µA. The flexible-shaped energy fiber showed promising mechanical and thermal stability. The entire efficiency remained at 88.2% after bending for 1,000 cycles and at 90.6% after 1,000 h of light

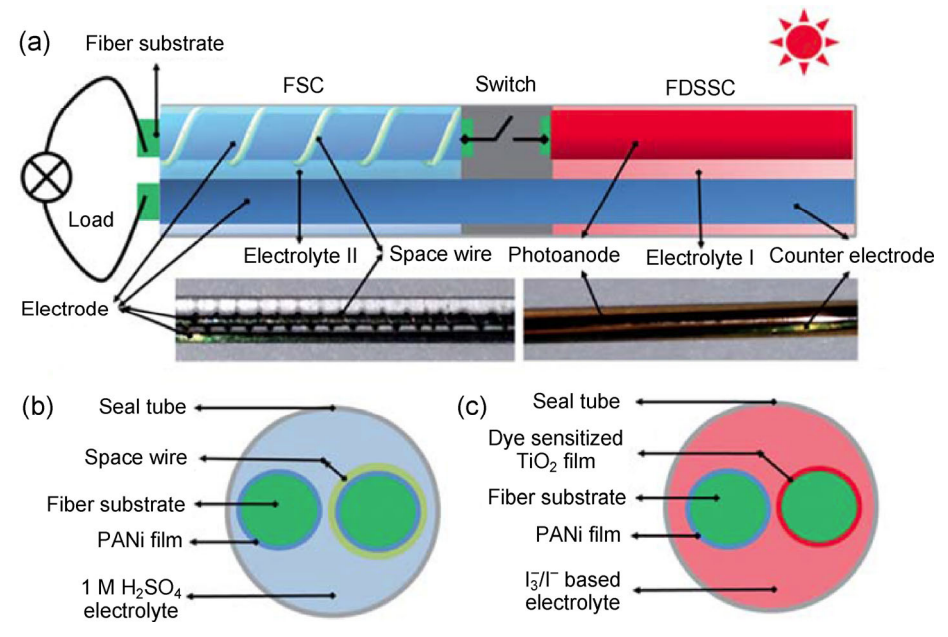


Figure 3 (a) Structural schematic and photograph of an integrated power fiber consisting of a fiber-shaped DSSC and a supercapacitor. (b) Cross-sectional schematic of the DSSC. Reproduced with permission from Ref. [38], © Royal Society of Chemistry 2013.

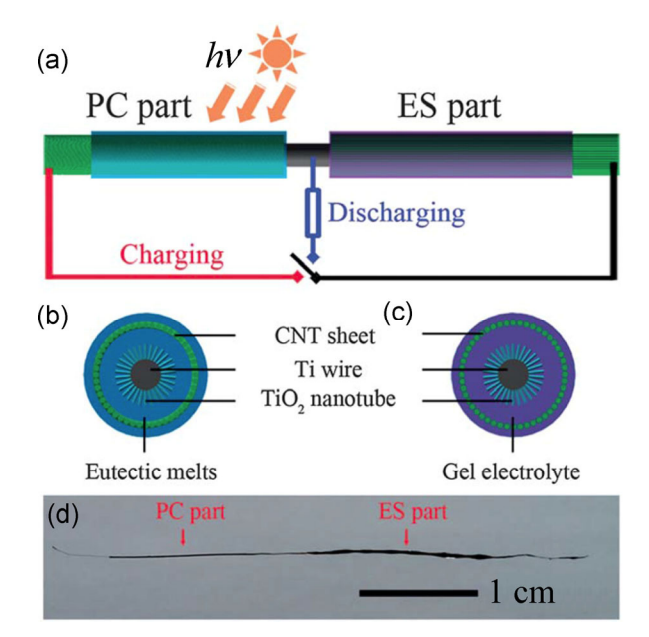


Figure 4 (a) Schematic of a core–shell elastic energy fiber with a DSSC and a supercapacitor. (b) and (c) Cross-section schematics of the DSSC and the supercapacitor, respectively. (d) Optical image of the energy fiber. Reproduced with permission from Ref. [58], © Royal Society of Chemistry 2014.

illumination. Regarding to the application of fibershaped devices in portable and wearable electronics, both the bending property and the stretching property have great influence on the performance. The aforementioned device was modified by fabricating a coaxial energy fiber that converted the solar energy in the shell and stored it in the core, instead of connecting the two separate parts [40]. An aligned CNT sheet was wrapped around an elastic rubber fiber acting as the internal electrode, followed by coating with a thin layer of PVA/H₃PO₄ gel as the electrolyte.

The device was completed into a supercapacitor with another CNT sheet wrapped outside the fiber. The fiber-shaped storage component was then inserted into an elastic plastic tube, outside of which was the DSSC part. This core-shell structure and aligned nanostructure at the interface resulted in a significantly improved PCE of 6.47% for the solar part, with a $I_{\rm sc}$ of 14.31 mA/cm², which was almost enhanced by a factor of 2. The overall efficiency of the elastic energy fiber was 1.83%, and it was well-maintained after bending and stretching. The photocharging and discharging processes were almost unaffected by bending at a radii of curvature ranging from 5 to 0.5 cm. The fiber device maintained a high performance after being stretched by 20%. With a far larger effective contact area and more efficient charge transport than the twisted structure, the coaxial structure enabled

the conversion of the solar energy into electrical energy in the sheath and stored the electrical energy in the core, resulting in high overall energy conversion and storage efficiencies with a good bending and stretching ability.

3.2 Integrated solar capacitors based on OSCs and supercapacitors

OSCs are photovoltaic devices fabricated via a solution process involving carbon-based organic semiconductors with large molecules. These solar cells are attractive owing to their advantages of a low cost, good mechanical flexibility, low weight, and tunable properties. They possess advantages over DSSCs for being all-solid state and compatible with roll-to-roll printing techniques on flexible substrates for large-scale production. An OSC is normally constructed on a bulk heterojunction involving donor–acceptor blends, having a transparent electrode/hole transporting layer/active layer/electron transporting layer/metal electrode structure. Single-junction and tandem OSCs with an efficiency higher than 10% have been frequently reported in recent years [10, 59–61].

A printable, all-solid state integrated solar capacitor was demonstrated by utilizing a single-walled CNT network as a common interface between the OSC and the supercapacitor [3]. P3HT was blended with [6,6]-phenyl-C₆₁-butyric acid methyl ester (PCBM) as the active layer. The CNT solution was drop-casted on top of the Al cathode, as well as the electrode of the supercapacitor, to form a CNT network as the integration platform (Fig. 5). The integrated device was less than 0.6 mm thick, weighed less than 1 g, and exhibited a 43% reduction in the internal resistance compared with the external wire-connected device. The OSC achieved a V_{oc} of 0.6 V and a PCE of 3.39%. After being photocharged for 70 s, the device exhibited a gravimetric specific capacitance of 28 F/g. By connecting two OSCs in series to charge the supercapacitor to the maximum storage capability, a capacitance of 79.8 F/g was achieved, which was almost three times of that for a single solar cell. Improving the photocharging voltage by connecting the solar cells in series is a general strategy for fully utilizing the energy-storage capacity of the supercapacitor, which is important for the output power

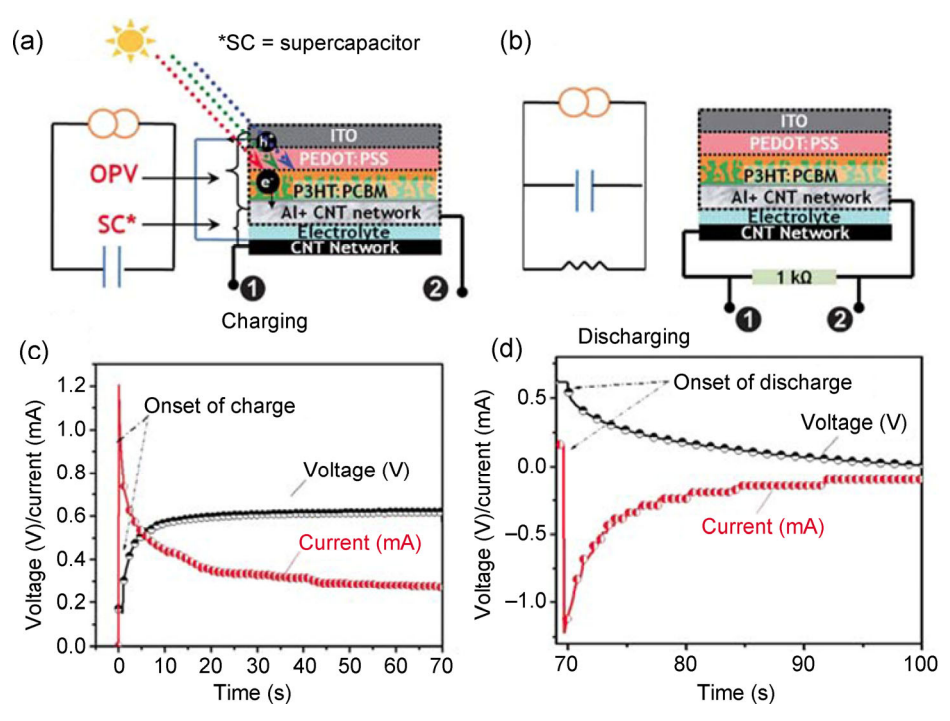


Figure 5 Schematic and circuit illustrations of a planar OSC-based integrated device during (a) the photocharging process and (b) the galvanostatic discharging process. Voltage/current–time profile for the (c) photocharging and (d) discharging processes of an OSC. Reproduced with permission from Ref. [3], © Royal Society of Chemistry 2013.

supply in applications in the modern electronics because most electronic devices are operated at several volts. The layer-by-layer architecture is compatible with the roll-to-roll printing process, creating opportunity for printed electronics.

Peng et al. developed a fiber-shaped, coaxial OSCsupercapacitor-integrated device [5]. The energy fiber was constructed with a Ti wire modified with TiO2 nanotube as the core and an aligned MWCNT sheet as the two electrodes. For the OSC part, the TiO2 nanotube-modified Ti wire was coated with P3HT:PCBM and PEDOT:poly (styrene sulfonate) (PSS), then the MWCNT sheet was wrapped around the surface as the cathode. The maximum PCE was 1.01%, obtained at a TiO₂ nanotube length of 1.8 μm, and 90% of this PCE was maintained after the device was placed in air for ten days. For the energy-storage part, MWCNT was wrapped on the same modified Ti wire, and then a PVA/H₃PO₄ electrolyte was injected between them. The linear specific capacitance was 0.077 mF/cm, with a stable energy-storage efficiency of 65.6%. The overall efficiency of the integrated fiber-shaped device was 0.82%. The all-solid-state device structure had good mechanical stability during bending deformation, retaining 90% of the efficiency after 1,000 bending cycles without sealing. Although the efficiency of the fiber device was lower than that of the planar one, the fiber device had unique advantages, such as being easily woven into flexible textiles.

A device integrating an OSC and a fully printed supercapacitor was recently optimized for indoor light energy harvesting [46]. The OSC was fabricated on glass with a classic structure using poly[N-9'heptadecanyl-2,7-carbazole-alt-5,5-(4,7-di-2-thienyl-2', 1',3'-benzothiadiazole)] (PCDTBT):[6,6]-phenyl- C_{71} butyric acid methyl ester (PC71BM) as active layer, where PEDOT:PSS and polyethylenimine ethoxylated (PEIE) were the hole- and electron-transporting layers, respectively. A PCE of 7.6% was achieved under simulated indoor light by optimization of the thickness of the PEIE layer, which decreased the dark current. The printed supercapacitor consisted of two carbon-black electrodes on a stainless-steel foil substrate and an ionic liquid electrolyte butylmethyl-imidazolium tetrafluoroborate (BMIM BF₄). The highest capacitance was 130 mF/cm² at a charge/ discharge rate of 0.25 mA/cm². The photo-rechargeable system yielded an overall efficiency of 1.56% under light irradiation of 1 sun. The indoor-optimal system achieved an overall efficiency of 2.92% when placed under indoor light for 3,090 s, exhibiting potential for autonomous application in various light conditions.

3.3 Integrated solar capacitors based on PVSCs and supercapacitors

PVSCs with hybrid inorganic-organic compounds $(CH_3NH_3PbX_3, X = Cl, Br, I)$ have been very promising in the photovoltaics field in the past few years, with efficiencies ranging from 3.8% to 22.1% [62–69]. Upon light illumination, the absorber becomes photoexcited, and carriers are created and driven towards the transport layer to be collected by the electrode. Because of the superior properties of perovskite—including a tunable bandgap, low-cost precursor materials, a high carrier mobility, and a simple solution or evaporation process-PVSC is superior to all of the other newgeneration solar cells. It was not until 2015 that the first use of a PVSC packed with energy-storage devices was reported [47]. A PVSC was fabricated with a structure of fluorine doped tin oxide (FTO)/ mesoporous-TiO₂/CH₃NH₃PbI₃/2,2',7,7'-tetrakis(N,Ndi-p-methoxyphenylamino)-9,9'-spirobifluorene (spiro-OMeTAD)/Au, which had a PCE of 13.6%. A symmetric supercapacitor with a bacterial-cellulose (BC) membrane/PPy/MWCNTs as the electrodes was used as the storage part. The supercapacitor had a maximum area specific capacitance of 572 mF/cm² at a discharge current of 1 mA/cm². Although the PVSC and the supercapacitor were associated simply by connecting the two devices in series using external lead wires, a very high overall energy conversion and storage efficiency of 10% was achieved for the first time, which originated from the high performance of the PVSC due to the resistance of the external connection. Notably, the first photocharging Li-ion battery using perovskite was demonstrated by directly packing four series-connected PVSCs with a battery, and a high efficiency of 7.80% was achieved with excellent cycling stability, outperforming the other reported solar battery systems [6]. With regard to their cost, efficiency, and fabrication process, PVSCs have far more promise for integrated solar capacitors than DSSCs and OSCs. For portable electronic applications, full integration without an external connection is always favorable.

Chai et al. fabricated co-anode and co-cathode solar capacitors by vertically integrating a PVSC with a MoO₃/Au/MoO₃ transparent electrode and a supercapacitor [28]. Their structures differed from all of the other integration systems. A semitransparent supercapacitor, which could automatically tune the optical transmittance of the device and store the electrochemical energy with the color change (Fig. 6), was installed on top of the PVSC. Regarding the coanode device, under light illumination, electrons were injected into the WO₃ cathode, and charges were then stored during the H⁺ insertion (WO₃ + H⁺ + e \rightarrow HWO₃). The electrode color changed from transparent to blue as the chemical state changed from +6 (bleached state) to +5 (color state). During the discharging process, the reversible H⁺ extraction released the charges $(HWO_3 \rightarrow WO_3 + H^+ + e)$, and the WO_3 film became transparent. As a result, the color of the energystorage part switched between blue and transparent during the photocharging and discharging. The energy density, power density, and areal capacitance of the co-anode devices were 13.4 mWh/m², 187.6 mW/m², and 286.8 F/m², respectively. These values were almost doubled for the co-cathode system. The tunable color state could also be an indicator of the amount of stored energy in the capacitor, which changed from semitransparent to dark blue with a reduction in the average visible transmission from 85% to 35.1% for the co-anode integrated devices during photocharging.

The photocharging was thus switched off automatically, as the dark color blocked most of the light. The smart design differs from all the previous reports in that it cannot only realize real-time indication of the energy stored and consumed but also improve the photostability by blocking the light once the capacitor is fully charged. This work expanded the integrated device for multifunctional smart windows, in addition to energy conversion and storage.

Fan et al. fabricated an integrated device with a twoelectrode structure based on PVSC and PEDOT/carbon supercapacitors [48]. The solar cell was constructed with an FTO/TiO₂/ZrO₂/mesoporous carbon electrode, where ClO₄-doped PEDOT was electrodeposited on the mesoporous carbon electrode before the electrode was filled with perovskite (MAPbI₃). Another PEDOTcarbon electrode was assembled against the counter electrode by a separator, along with an electrolyte composed of LiClO₄ and CH₃NH₃I (MAI) in isopropanol, which acted as the supercapacitor. The MAI served as the stabilizer for the MAPBI₃. The PVCS in its integrated form exhibited a $J_{\rm sc}$ of 18.62 mA/cm², a $V_{\rm oc}$ of 0.71 V, an FF of 0.48, and a PCE of 6.37%, well matching the single device. The capacitance of the supercapacitor remained at 95% after 2,000 charge/ discharge cycles. The energy density was calculated to be 0.783 mWh/cm² at a discharge current of 1 mA/cm². The overall efficiency reached its maximum of 4.7% within 1 s with an energy-storage efficiency of 73.77%. Although this configuration indeed improves the integration of the two energy parts and facilitates real applications, the efficiency is largely limited by the

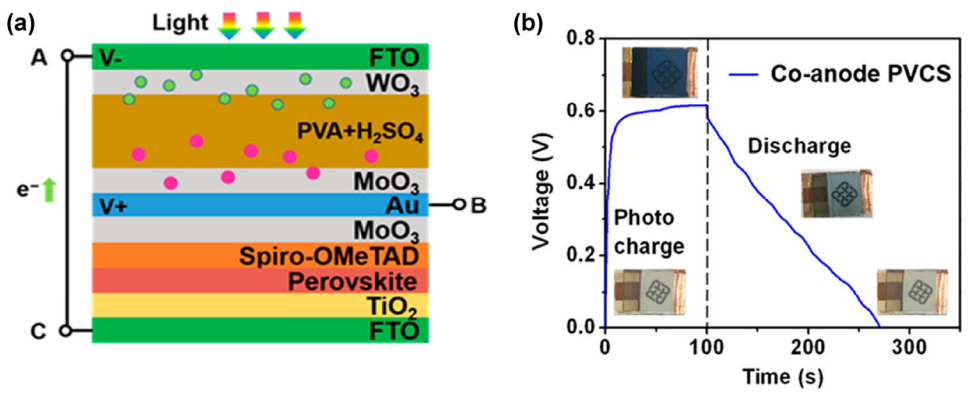


Figure 6 (a) Schematic of the co-anode, PVSC-based transparent integrated device. (b) Voltage–time curves of the co-anode PVCS device for the photocharging process within 100 s and the discharging process at a current density of 0.1 mA/cm², along with the color change of the device during different processes. Reproduced with permission from Ref. [28], © American Chemical Society 2016.

poor performance of the PVSC. Additionally, the work function of PEDOT decreased as the doping content increased under oxidation, which the researchers attributed to the dipole effect of the positive and negative charges located in the thin film.

4 Conclusions and prospects

We provided a brief overview of integrated solar capacitors that combine solar cells and supercapacitors as self-powering units. We focused on different new-generation solar energy conversion parts, i.e., DSSCs, PSCs, and PVSCs, with planar or fiber-shaped configurations. Excellent properties, such as flexibility, stability, intelligence, and transparency, have been demonstrated in integrated systems, which largely expand the applications of these devices in functional textiles or portable electronics. The overall efficiencies have exceeded 10% owing to the emergence of higherficiency PVSCs and supercapacitors. Other combinations also show good performance with specific characteristics.

Although considerable progress has been made in this promising research field, the device performance is still low compared with that of the commercial inorganic counterparts and is far from the level needed for application in powering real electronics. The planar devices have a facile fabrication process and high efficiency but a rigid configuration that limits their applications. In contrast, fiber-shaped integrated solar capacitors are flexible and weavable but have a lower performance and complicated fabrication process. Another bottleneck for fiber-shaped devices is that their high resistance degrades their efficiency, which raises the demand for a highly conductive fiber electrode. On the device level, the efficiency of the solar-cell part should be as high as possible, and the supercapacitor should be well matched to decrease the energy loss during the energy storage, with consideration of the electrode materials, the size of the energy parts, and the stability. The supercapacitor should be fully charged very quickly by the solar cell because the energy-storage capability is very low. Thus, strategies for power management to balance the energy generation and consumption and for improving the capacity of the supercapacitor or using batteries with a high power density are necessary. To overcome the leakage problem of the DSSC-based solar capacitor, all-solid state devices are required. Integration of the planar devices can be accomplished on flexible substrates that allow for the printable or roll-to-roll process, which facilitates large-scale production and feasibility.

Acknowledgements

This work was supported by the National Key Research and Development Program of China (No. 2016YFA0202402), the National Natural Science Foundation of China (Nos. 91123005 and 61674108), the Priority Academic Program Development of Jiangsu Higher Education Institutions (PAPD), and Collaborative Innovation Center of Suzhou Nano Science and Technology.

References

- Miyasaka, T.; Murakami, T. N. The photocapacitor: An efficient self-charging capacitor for direct storage of solar energy. *Appl. Phys. Lett.* 2004, 85, 3932–3934.
- [2] Bae, J.; Park, Y. J.; Lee, M.; Cha, S. N.; Choi, Y. J.; Lee, C. S.; Kim, J. M.; Wang, Z. L. Single-fiber-based hybridization of energy converters and storage units using graphene as electrodes. *Adv. Mater.* 2011, 23, 3446–3449.
- [3] Wee, G.; Salim, T.; Lam, Y. M.; Mhaisalkar, S. G.; Srinivasan, M. Printable photo-supercapacitor using singlewalled carbon nanotubes. *Energy Environ. Sci.* 2011, 4, 413–416.
- [4] Guo, W. X.; Xue, X. Y.; Wang, S. H.; Lin, C. J.; Wang, Z. L. An integrated power pack of dye-sensitized solar cell and Li battery based on double-sided TiO₂ nanotube arrays. *Nano Lett.* 2012, 12, 2520–2523.
- [5] Zhang, Z. T.; Chen, X. L.; Chen, P. N.; Guan, G. Z.; Qiu, L. B.; Lin, H. J.; Yang, Z. B.; Bai, W. Y.; Luo, Y. F.; Peng, H. S. Integrated polymer solar cell and electrochemical supercapacitor in a flexible and stable fiber format. *Adv. Mater.* 2014, 26, 466–470.
- [6] Xu, J. T.; Chen, Y. H.; Dai, L. M. Efficiently photo-charging lithium-ion battery by perovskite solar cell. *Nat. Commun.* 2015, 6, 8103.
- [7] Chen, J.; Huang, Y.; Zhang, N. N.; Zou, H. Y.; Liu, R. Y.; Tao, C. Y.; Fan, X.; Wang, Z. L. Micro-cable structured textile for simultaneously harvesting solar and mechanical

- energy. Nat. Energy 2016, 1, 16138.
- [8] Law, M.; Greene, L. E.; Johnson, J. C.; Saykally, R.; Yang, P. D. Nanowire dye-sensitized solar cells. *Nat. Mater.* 2005, 4, 455–459.
- [9] Ma, W.; Yang, C.; Gong, X.; Lee, K.; Heeger, A. J. Thermally stable, efficient polymer solar cells with nanoscale control of the interpenetrating network morphology. *Adv. Funct. Mater.* 2005, 15, 1617–1622.
- [10] Chen, H.-Y.; Hou, J. H.; Zhang, S. Q.; Liang, Y. Y.; Yang, G. W.; Yang, Y.; Yu, L. P.; Wu, Y.; Li, G. Polymer solar cells with enhanced open-circuit voltage and efficiency. *Nat. Photonics* 2009, *3*, 649–653.
- [11] Hagfeldt, A.; Boschloo, G.; Sun, L. C.; Kloo, L.; Pettersson, H. Dye-sensitized solar cells. *Chem. Rev.* 2010, 110, 6595–6663.
- [12] Lee, M. M.; Teuscher, J.; Miyasaka, T.; Murakami, T. N.; Snaith, H. J. Efficient hybrid solar cells based on mesosuperstructured organometal halide perovskites. *Science* 2012, 338, 643–647.
- [13] Li, G.; Zhu, R.; Yang, Y. Polymer solar cells. *Nat. Photonics* **2012**, *6*, 153–161.
- [14] Liu, M. Z.; Johnston, M. B.; Snaith, H. J. Efficient planar heterojunction perovskite solar cells by vapour deposition. *Nature* 2013, 501, 395–398.
- [15] He, Z. C.; Xiao, B.; Liu, F.; Wu, H. B.; Yang, Y. L.; Xiao, S.; Wang, C.; Russell, T. P.; Cao, Y. Single-junction polymer solar cells with high efficiency and photovoltage. *Nat. Photonics* 2015, 9, 174–179.
- [16] Jeon, N. J.; Noh, J. H.; Yang, W. S.; Kim, Y. C.; Ryu, S.; Seo, J.; Seok, S. I. Compositional engineering of perovskite materials for high-performance solar cells. *Nature* 2015, 517, 476–480.
- [17] Nie, W. Y.; Tsai, H.; Asadpour, R.; Blancon, J.-C.; Neukirch, A. J.; Gupta, G.; Crochet, J. J.; Chhowalla, M.; Tretiak, S.; Alam, M. A. et al. High-efficiency solution-processed perovskite solar cells with millimeter-scale grains. *Science* 2015, 347, 522–525.
- [18] Liu, R. Y.; Lee, S. T.; Sun, B. Q. 13.8% efficiency hybrid Si/organic heterojunction solar cells with MoO₃ film as antireflection and inversion induced layer. *Adv. Mater.* **2014**, *26*, 6007–6012.
- [19] Winter, M.; Brodd, R. J. What are batteries, fuel cells, and supercapacitors? *Chem. Rev.* **2004**, *104*, 4245–4270.
- [20] Yang, Z. G.; Zhang, J. L.; Kintner-Meyer, M. C. W.; Lu, X. C.; Choi, D.; Lemmon, J. P.; Liu, J. Electrochemical energy storage for green grid. *Chem. Rev.* 2011, 111, 3577–3613.
- [21] Zhang, L. L.; Zhao, X. S. Carbon-based materials as supercapacitor electrodes. *Chem. Soc. Rev.* 2009, 38, 2520– 2531.

- [22] Chen, S.; Zhu, J. W.; Wu, X. D.; Han, Q. F.; Wang, X. Graphene oxide-MnO₂ nanocomposites for supercapacitors. *ACS Nano* **2010**, *4*, 2822–2830.
- [23] Wang, H. L.; Holt, C. M. B.; Li, Z.; Tan, X. H.; Amirkhiz, B. S.; Xu, Z. W.; Olsen, B. C.; Stephenson, T.; Mitlin, D. Graphene-nickel cobaltite nanocomposite asymmetrical supercapacitor with commercial level mass loading. *Nano Res.* 2012, 5, 605–617.
- [24] Peng, M.; Zou, D. C. Flexible fiber/wire-shaped solar cells in progress: Properties, materials, and designs. *J. Mater. Chem. A* 2015, 3, 20435–20458.
- [25] Wang, X. F.; Jiang, K.; Shen, G. Z. Flexible fiber energy storage and integrated devices: Recent progress and perspectives. *Mater. Today* **2015**, *18*, 265–272.
- [26] Huang, Q. Y.; Wang, D. R.; Zheng, Z. J. Textile-based electrochemical energy storage devices. *Adv. Energy Mater*. 2016, 6, 1600783.
- [27] Huang, Y.; Zhu, M. S.; Huang, Y.; Pei, Z. X.; Li, H. F.; Wang, Z. F.; Xue, Q.; Zhi, C. Y. Multifunctional energy storage and conversion devices. *Adv. Mater.* 2016, 28, 8344–8364.
- [28] Zhou, F. C.; Ren, Z. W.; Zhao, Y. D.; Shen, X. P.; Wang, A. W.; Li, Y. Y.; Surya, C.; Chai, Y. Perovskite photovoltachromic supercapacitor with all-transparent electrodes. ACS Nano 2016, 10, 5900–5908.
- [29] Chen, T.; Qiu, L. B.; Yang, Z. B.; Cai, Z. B.; Ren, J.; Li, H. P.; Lin, H. J.; Sun, X. M.; Peng, H. S. An integrated "energy wire" for both photoelectric conversion and energy storage. *Angew. Chem., Int. Ed.* 2012, 51, 11977–11980.
- [30] Xu, J.; Wu, H.; Lu, L. F.; Leung, S. F.; Chen, D.; Chen, X. Y.; Fan, Z. Y.; Shen, G. Z.; Li, D. D. Integrated photosupercapacitor based on Bi-polar TiO₂ nanotube arrays with selective one-side plasma-assisted hydrogenation. *Adv. Funct. Mate.* 2014, 24, 1840–1846.
- [31] Hodes, G.; Manassen, J.; Cahen, D. Photoelectrochemical energy conversion and storage using polycrystalline chalcogenide electrodes. *Nature* 1976, 261, 403–404.
- [32] O'Regan, B.; Grätzel, M. A low-cost, high-efficiency solar cell based on dye-sensitized colloidal TiO₂ films. *Nature* **1991**, *353*, 737–740.
- [33] Matsui, T.; Sai, H.; Saito, K.; Kondo, M. High-efficiency thin-film silicon solar cells with improved light-soaking stability. *Prog. Photovolt.: Res. Appl.* **2013**, *21*, 1363–1369.
- [34] Green, M. A.; Emery, K.; Hishikawa, Y.; Warta, W.; Dunlop, E. D. Solar cell efficiency tables (Version 45). *Prog. Photovolt.: Res. Appl.* 2015, 23, 1–9.
- [35] Kakiage, K.; Aoyama, Y.; Yano, T.; Oya, K.; Fujisawa, J.-I.; Hanaya, M. Highly-efficient dye-sensitized solar cells with collaborative sensitization by silyl-anchor and carboxy-anchor dyes. *Chem. Commun.* 2015, 51, 15894–15897.

- [36] Murakami, T. N.; Kawashima, N.; Miyasaka, T. A high-voltage dye-sensitized photocapacitor of a three-electrode system. *Chem. Commun.* 2005, 3346–3348.
- [37] Hsu, C.-Y.; Chen, H.-W.; Lee, K.-M.; Hu, C.-W.; Ho, K.-C. A dye-sensitized photo-supercapacitor based on PProDOT-Et₂ thick films. *J. Power Sources* 2010, 195, 6232–6238.
- [38] Fu, Y. P.; Wu, H. W.; Ye, S. Y.; Cai, X.; Yu, X.; Hou, S. C.; Kafafy, H.; Zou, D. C. Integrated power fiber for energy conversion and storage. *Energy Environ. Sci.* 2013, 6, 805–812.
- [39] Yang, Z. B.; Li, L.; Luo, Y. F.; He, R. X.; Qiu, L. B.; Lin, H. J.; Peng, H. S. An integrated device for both photoelectric conversion and energy storage based on free-standing and aligned carbon nanotube film. *J. Mater. Chem. A* 2013, 1, 954–958.
- [40] Yang, Z. B.; Deng, J.; Sun, H.; Ren, J.; Pan, S. W.; Peng, H. S. Self-powered energy fiber: Energy conversion in the sheath and storage in the core. Adv. Mater. 2014, 26, 7038–7042.
- [41] Cohn, A. P.; Erwin, W. R.; Share, K.; Oakes, L.; Westover, A. S.; Carter, R. E.; Bardhan, R.; Pint, C. L. All silicon electrode photocapacitor for integrated energy storage and conversion. *Nano Lett.* 2015, 15, 2727–2731.
- [42] Hauch, A.; Georg, A.; Krašovec, U. O.; Orel, B. Photovoltaically self-charging battery. J. Electrochem. Soc. 2002, 149, A1208–A1211.
- [43] Liu, P.; Cao, Y. L.; Li, G. R.; Gao, X. P.; Ai, X. P.; Yang, H. X. A solar rechargeable flow battery based on photoregeneration of two soluble redox couples. *ChemSusChem* 2013, 6, 802–806.
- [44] Zhang, X.; Huang, X. Z.; Li, C. S.; Jiang, H. R. Dyesensitized solar cell with energy storage function through PVDF/ZnO nanocomposite counter electrode. *Adv. Mater.* 2013, 25, 4093–4096.
- [45] Chen, H.-W.; Hsu, C.-Y.; Chen, J.-G.; Lee, K.-M.; Wang, C.-C.; Huang, K.-C.; Ho, K.-C. Plastic dye-sensitized photo-supercapacitor using electrophoretic deposition and compression methods. *J. Power Sources* 2010, 195, 6225–6231.
- [46] Lechêne, B. P.; Cowell, M.; Pierre, A.; Evans, J. W.; Wright, P. K.; Arias, A. C. Organic solar cells and fully printed super-capacitors optimized for indoor light energy harvesting. *Nano Energy* 2016, 26, 631–640.
- [47] Xu, X. B.; Li, S. H.; Zhang, H.; Shen, Y.; Zakeeruddin, S. M.; Graetzel, M.; Cheng, Y.-B.; Wang, M. K. A power pack based on organometallic perovskite solar cell and supercapacitor. ACS Nano 2015, 9, 1782–1787.
- [48] Xu, J.; Ku, Z. L.; Zhang, Y. Q.; Chao, D. L.; Fan, H. J. Integrated photo-supercapacitor based on pedot modified

- printable perovskite solar cell. *Adv. Mater. Technol.* **2016**, 1, 1600074.
- [49] Zhang, M.; Zhou, Q. Q.; Chen, J.; Yu, X. W.; Huang, L.; Li, Y. R.; Li, C.; Shi, G. Q. An ultrahigh-rate electrochemical capacitor based on solution-processed highly conductive PEDOT:PSS films for AC line-filtering. *Energy Environ*. Sci. 2016, 9, 2005–2010.
- [50] Snook, G. A.; Kao, P.; Best, A. S. Conducting-polymer-based supercapacitor devices and electrodes. *J. Power Sources* **2011**, *196*, 1–12.
- [51] Zhang, X. J.; Shi, W. H.; Zhu, J. X.; Zhao, W. Y.; Ma, J.; Mhaisalkar, S.; Maria, T. L.; Yang, Y. H.; Zhang, H.; Hng, H. H. et al. Synthesis of porous NiO nanocrystals with controllable surface area and their application as supercapacitor electrodes. *Nano Res.* 2010, *3*, 643–652.
- [52] Wang, H. L.; Liang, Y. Y.; Mirfakhrai, T.; Chen, Z.; Casalongue, H. S.; Dai, H. J. Advanced asymmetrical supercapacitors based on graphene hybrid materials. *Nano Res.* 2011, 4, 729–736.
- [53] Lu, X. H.; Zhai, T.; Zhang, X. H.; Shen, Y. Q.; Yuan, L. Y.; Hu, B.; Gong, L.; Chen, J.; Gao, Y. H.; Zhou, J. et al. WO_{3-x}@Au@MnO₂ core–shell nanowires on carbon fabric for high-performance flexible supercapacitors. *Adv. Mater.* 2012, 24, 938–944.
- [54] Kaempgen, M.; Chan, C. K.; Ma, J.; Cui, Y.; Gruner, G. Printable thin film supercapacitors using single-walled carbon nanotubes. *Nano Lett.* 2009, 9, 1872–1876.
- [55] Shi, C. L.; Dong, H.; Zhu, R.; Li, H.; Sun, Y. C.; Xu, D. S.; Zhao, Q.; Yu, D. P. An "all-in-one" mesh-typed integrated energy unit for both photoelectric conversion and energy storage in uniform electrochemical system. *Nano Energy* 2015, 13, 670–678.
- [56] Skunik-Nuckowska, M.; Grzejszczyk, K.; Kulesza, P. J.; Yang, L.; Vlachopoulos, N.; Häggman, L.; Johansson, E.; Hagfeldt, A. Integration of solid-state dye-sensitized solar cell with metal oxide charge storage material into photoelectrochemical capacitor. *J. Power Sources* 2013, 234, 91–99.
- [57] Zheng, J. P.; Cygan, P. J.; Jow, T. R. Hydrous ruthenium oxide as an electrode material for electrochemical capacitors. *J. Electrochem. Soc.* 1995, 142, 2699–2703.
- [58] Chen, X. L.; Sun, H.; Yang, Z. B.; Guan, G. Z.; Zhang, Z. T.; Qiu, L. B.; Peng, H. S. A novel "energy fiber" by coaxially integrating dye-sensitized solar cell and electrochemical capacitor. *J. Mater. Chem. A* 2014, 2, 1897–1902.
- [59] Chen, J. D.; Cui, C. H.; Li, Y. Q.; Zhou, L.; Ou, Q. D.; Li, C.; Li, Y. F.; Tang, J. X. Single-junction polymer solar cells exceeding 10% power conversion efficiency. *Adv. Mater.* 2015, 27, 1035–1041.

Nano Res.

[60] Liu, C.; Yi, C.; Wang, K.; Yang, Y. L.; Bhatta, R. S.; Tsige, M.; Xiao, S. Y.; Gong, X. Single-junction polymer solar cells with over 10% efficiency by a novel twodimensional donor-acceptor conjugated copolymer. ACS Appl. Mater. Interfaces 2015, 7, 4928–4935.

- [61] Zhou, H. Q.; Zhang, Y.; Mai, C. K.; Collins, S. D.; Bazan, G. C.; Nguyen, T. Q.; Heeger, A. J. Polymer homo-tandem solar cells with best efficiency of 11.3%. *Adv. Mater.* 2015, 27, 1767–1773.
- [62] Kojima, A.; Teshima, K.; Shirai, Y.; Miyasaka, T. Organometal halide perovskites as visible-light sensitizers for photovoltaic cells. J. Am. Chem. Soc. 2009, 131, 6050– 6051.
- [63] Ball, J. M.; Lee, M. M.; Hey, A.; Snaith, H. J. Low-temperature processed meso-superstructured to thin-film perovskite solar cells. *Energy Environ. Sci.* 2013, 6, 1739–1743.
- [64] Bai, S.; Wu, Z. W.; Wu, X. J.; Jin, Y. Z.; Zhao, N.; Chen, Z. H.; Mei, Q. Q.; Wang, X.; Ye, Z. Z.; Song, T. et al. High-performance planar heterojunction perovskite solar cells: Preserving long charge carrier diffusion lengths and interfacial engineering. *Nano Res.* 2014, 7, 1749–1758.
- [65] Im, J.-H.; Jang, I.-H.; Pellet, N.; Grätzel, M.; Park, N.-G.

- Growth of CH₃NH₃PbI₃ cuboids with controlled size for high-efficiency perovskite solar cells. *Nat. Nanotechnol.* **2014**, *9*, 927–932.
- [66] Ahn, N.; Son, D.-Y.; Jang, I.-H.; Kang, S. M.; Choi, M.; Park, N.-G. Highly reproducible perovskite solar cells with average efficiency of 18.3% and best efficiency of 19.7% fabricated via lewis base adduct of lead(II) iodide. *J. Am. Chem. Soc.* 2015, 137, 8696–8699.
- [67] Chen, W.; Wu, Y. Z.; Yue, Y. F.; Liu, J.; Zhang, W. J.; Yang, X. D.; Chen, H.; Bi, E. B.; Ashraful, I.; Grätzel, M. et al. Efficient and stable large-area perovskite solar cells with inorganic charge extraction layers. *Science* 2015, 350, 944–948.
- [68] Jacobsson, T. J.; Correa-Baena, J.-P.; Pazoki, M.; Saliba, M.; Schenk, K.; Grätzel, M.; Hagfeldt, A. Exploration of the compositional space for mixed lead halogen perovskites for high efficiency solar cells. *Energy Environ. Sci.* 2016, 9, 1706–1724.
- [69] Li, X.; Bi, D. Q.; Yi, C. Y.; Décoppet, J.-D.; Luo, J. S.; Zakeeruddin, S. M.; Hagfeldt, A.; Grätzel, M. A vacuum flash-assisted solution process for high-efficiency large-area perovskite solar cells. *Science* 2016, 353, 58–62.